

Development & Validation of Low-Cost, Highly-Durable, Spinel-Based Materials for SOFC Cathode-Side Contact

Jiahong Zhu

**Department of Mechanical Engineering
Tennessee Technological University (TTU)**

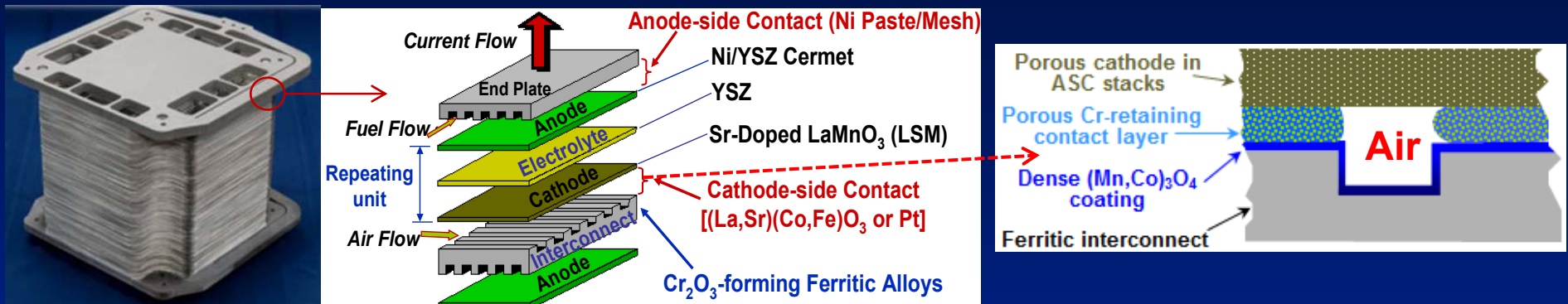
***20th Annual Solid Oxide Fuel Cell (SOFC) Project Review Meeting
April 29-May 1, 2019***

Outline

- **Introduction and Project Objectives**
- **Effect of Spinel Compositions on the Electrical Conductivity and CTE**
- **Performance Evaluation of the Sintered Spinel Contact Thermally Converted from Metallic Precursors**
 - Area Specific Resistance (ASR), Chemical Compatibility, etc.
- **Reactive Sintering of Dense $(\text{Mn,Co})_3\text{O}_4$ Coatings**
- **Co-sintering of Spinel-Based Coating/Contact Dual-Layer Structure**
- **Concluding Remarks**
- **Acknowledgments**

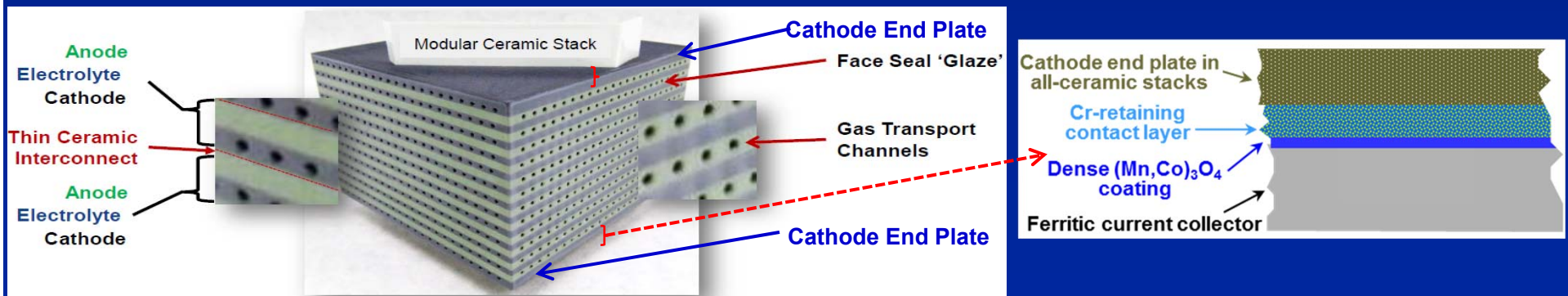
Need of Contacting for Different SOFC Stacks

- In stacks with anode-supported cells (ASC-SOFC), the contact is required to minimize the cathode-interconnect interfacial resistance.



Cathode-Interconnect Interface in ASC SOFC Stacks

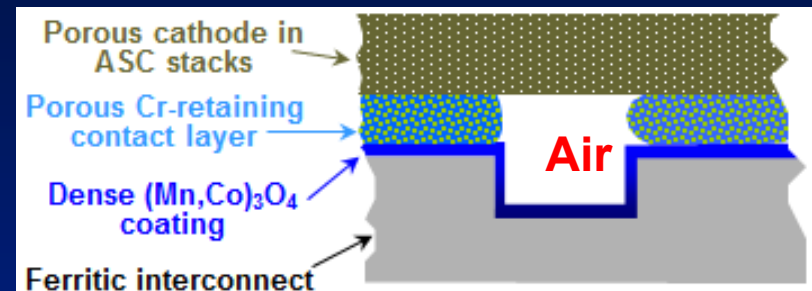
- In all-ceramic stacks, the contact is required to minimize the interfacial resistance between the current collector plate and cathode end plate.



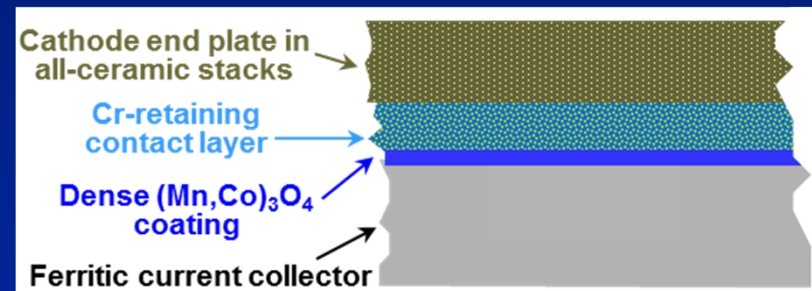
Cathode-Current Collector Interface in All-Ceramic SOFC Stacks

Contact Material Requirements

- Requirements for contact materials in ASC-SOFC and all-ceramic SOFC stacks are generally similar, including:
 - Low material/processing cost
 - High electrical conductivity
 - Match in coefficient of thermal expansion (CTE)
 - Adequate stability and compatibility
 - Appropriate sinterability
 - Good bonding strength with adjacent stack components
 - Absence of volatile species
- Additionally, a reasonable porosity level in the cathode-side contact is needed in ASC stacks for maximizing the triple phase boundaries for cathodic reaction.



Cathode-Interconnect Interface in ASC-SOFC Stacks



Cathode-Current Collector Interface in All-Ceramic SOFC Stacks

Different Contact Materials

- While various materials for ferritic alloy-cathode contacting have been studied, most developments have focused on $(\text{La}, \text{Sr})(\text{Mn}, \text{Co}, \text{Fe}, \text{Ni}, \text{Cu})\text{O}_3$:
 - Difficulty in balancing the electrical conductivity, CTE, sinterability and chemical compatibility of the perovskites.

Material Type	Example	CTE ($\times 10^{-6} / \text{K}$) (20–800°C)	Conductivity ($\text{S}\cdot\text{cm}^{-1}$, 800°C)	Main Concern
Noble Metal	Pt	10.0	Metallic	High Cost
	Pd	12.3	Metallic	High Cost
	Au	16.6	Metallic	High Cost
	Ag	22.0	Metallic	Volatility
Perovskite	$(\text{La}_{0.8}\text{Sr}_{0.2})\text{CoO}_{3-\delta}$	19.2 (20-1000°C)	1400	CTE Mismatch
	$(\text{La}_{0.8}\text{Sr}_{0.2})(\text{Co}_{0.5}\text{Fe}_{0.5})\text{O}_{3-\delta}$	18.3 (20-1000°C)	340	CTE Mismatch
	$(\text{La}_{0.8}\text{Sr}_{0.2})(\text{Co}_{0.5}\text{Mn}_{0.5})\text{O}_{3-\delta}$	15.0 (20-1000°C)	190	CTE Mismatch
	$(\text{La}_{0.8}\text{Sr}_{0.2})\text{MnO}_3$	11.7 (20-1000°C)	170	Sinterability
	$\text{LaMn}_{0.45}\text{Co}_{0.35}\text{Cu}_{0.2}\text{O}_3$	13.9	80	Mn/Cu Migration
Spinel	MnCo_2O_4	9.7-14.4	24- 89	Sinterability
	$\text{Mn}_{1.5}\text{Co}_{1.5}\text{O}_4$	10.6-11.6	55-68	Sinterability
	NiCo_2O_4	12.1	0.93	Sinterability
	NiFe_2O_4	11.8	0.3, 6.8, 17.1	Sinterability
	$\text{Ni}_{0.85}\text{Fe}_{2.15}\text{O}_4$	12.1	15.4	Sinterability

Why (Ni,Fe)₃O₄- and (Mn,Co)₃O₄-Based Spinel as Contact Material?

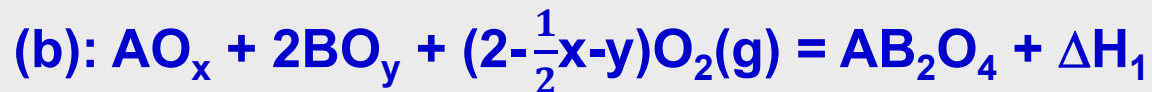
- Conductive spinels based on (Ni,Fe)₃O₄ and (Mn,Co)₃O₄, which have been extensively evaluated as interconnect coating, are also promising for contact application, based on electrical conductivity, CTE, chemical compatibility, etc.

Material Type	Example	CTE ($\times 10^{-6}$ /K) (20–800°C)	Conductivity (S·cm ⁻¹ , 800°C)	Main Concern
Spinel	MnCo ₂ O ₄	9.7-14.4	24- 89	Sinterability
	Mn _{1.5} Co _{1.5} O ₄	10.6-11.6	55-68	Sinterability
	NiCo ₂ O ₄	12.1	0.93	Sinterability
	NiFe ₂ O ₄	11.8	0.3, 6.8, 17.1	Sinterability
	Ni _{0.85} Fe _{2.15} O ₄	12.1	15.4	Sinterability

- Unfortunately, the sinterability of spinels is very poor (typically $\geq 1000^\circ\text{C}$), if metal oxides are used as the starting powders.
- Employment of **metallic powders** (instead of oxide powders) as the starting precursor will lower the sintering temperature via a reactive sintering mechanism called **eenvironmentally-assisted rreactive sintering (EARS).**

Utilization of EARS for Reduced-Temperature Sintering of Spinel-Based Contact

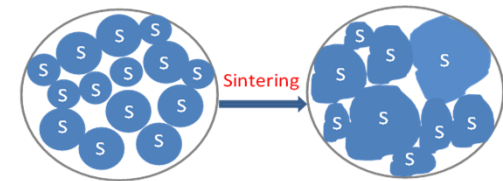
- In EARS, with the participation of oxygen from air, the **metallic powder precursor** will be oxidized and reacted to form a well-sintered spinel at a reduced temperature (e.g., 900°C):



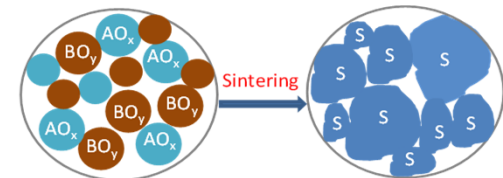
$$\Delta H_3 > \Delta H_2 \gg \Delta H_1$$

- Enhanced sintering via EARS is likely due to:
 - Heat released during the reaction;
 - Volume expansion upon conversion of metal to metal oxide;
 - Formation of highly-active surface nano-oxides;
 - Shorter diffusion distance when a pre-alloyed powder is employed.

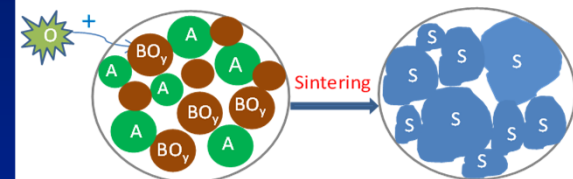
Zhu et al., IJHE, 2018



(a) with a spinel (S) powder



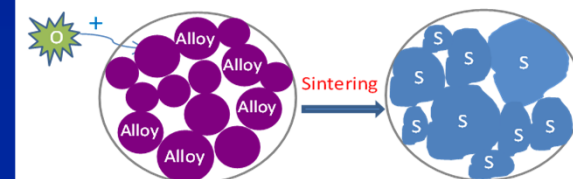
(b) with a mixture of metal oxides



(c) with metal and oxide powders



(d) With two metal powders

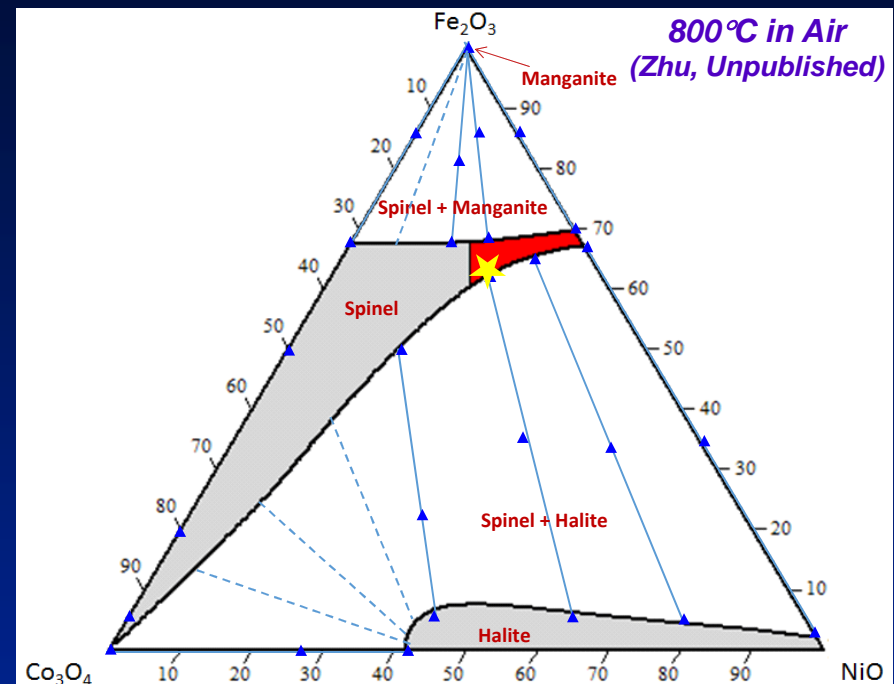
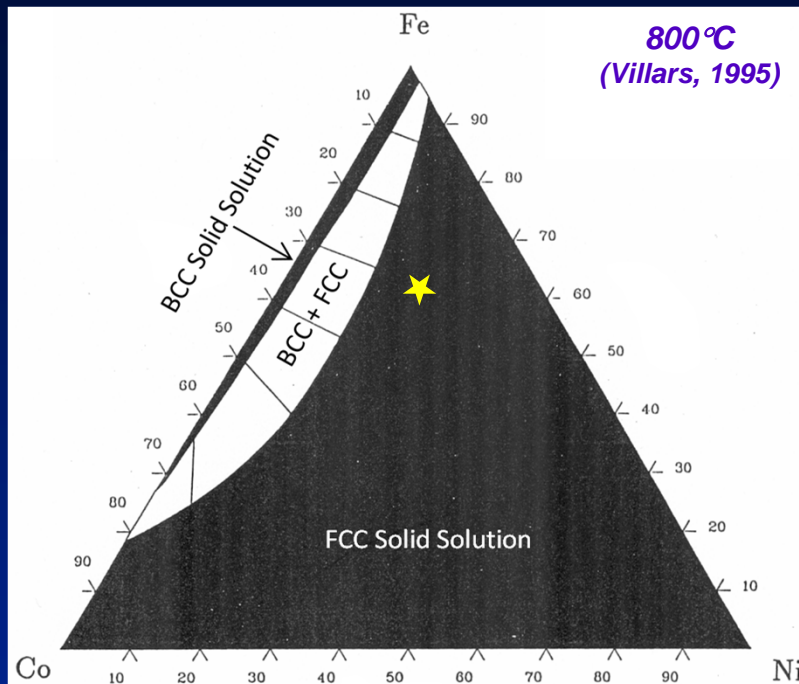


(e) With a pre-alloyed powder

Project Objectives

- **Optimization of the multi-component alloy precursor composition as contact material.** The alloy compositions will be optimized via composition screening in the $(\text{Ni,Fe,Co,X})_3\text{O}_4$ and $(\text{Mn,Co,X})_3\text{O}_4$ system, alloy design using physical metallurgy principles, and cost considerations. The desired alloy powders will be manufactured & characterized in detail.
- **Demonstration/validation of the contact layer performance in relevant SOFC stack environments.** Long-term ASR behavior and in-stack performance of the contact layer in relevant stack operating environments, its microstructure, chemical compatibility & Cr-retaining capability will be evaluated.
- **Further cost reduction and commercialization assessment.** Approaches to further reducing the stack cost will be explored, such as co-sintering of the interconnect coating and contact layer. Cost analysis and scale-up assessment will be conducted for potential commercialization.

Phase Equilibria in Co_3O_4 - Fe_2O_3 - NiO System



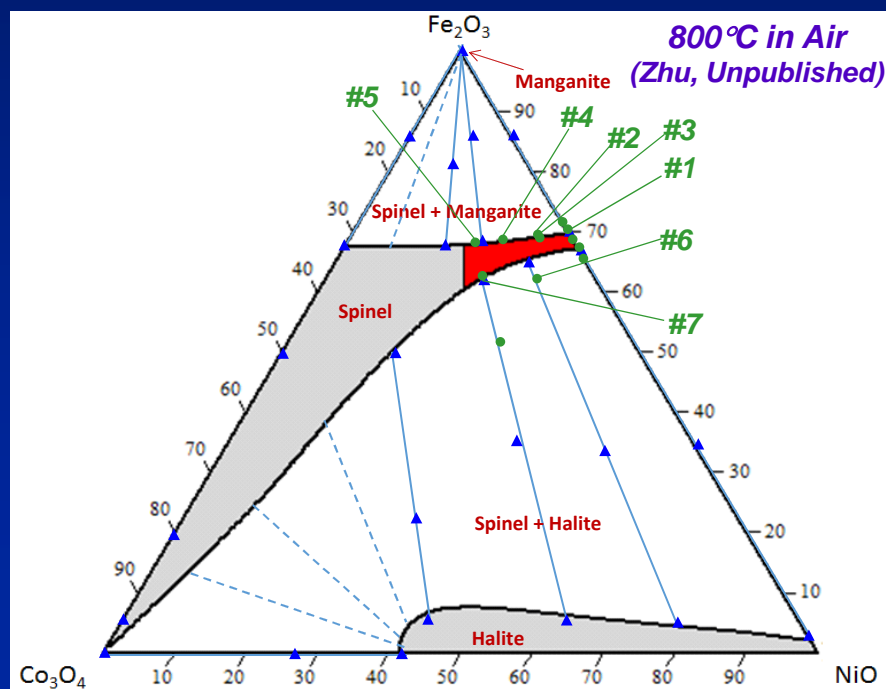
- While the phase equilibria in ternary Fe-Ni-Co system have been well documented, this is not the case for the Fe-Ni-Co-O system.
- By combining the binary system data, thermodynamic assessment, & experimental investigation, we have determined the Fe_2O_3 - NiO - Co_3O_4 phase diagram at 800°C in air.
- Of particular interest to our contact material development are the low-Co spinel compositions near the spinel phase boundaries.

Spinel Compositional Optimization in $(\text{Ni,Fe,Co,X})_3\text{O}_4$

- The pellets of various $(\text{Ni,Fe,Co,X})_3\text{O}_4$ spinel compositions were prepared for electrical conductivity and CTE measurements.
- The Fe/Ni/Co ratio in $(\text{Ni,Fe,Co})_3\text{O}_4$ was varied, while keeping the overall composition close to the phase boundaries.
- Additional microalloying elements ($X = X', X''$, etc. – transitional metal and/or a reactive element) were doped into $(\text{Ni,Fe,Co})_3\text{O}_4$ to further improve its properties.

Selected Compositions Evaluated in Our Study

Sample #	Composition
1	$\text{Ni}_{.84}\text{Fe}_{2.16}\text{O}_4$
2	$\text{Ni}_{.69}\text{Co}_{.15}\text{Fe}_{2.16}\text{O}_4$
3	$\text{Ni}_{.72}\text{Co}_{.15}\text{Fe}_{2.13}\text{O}_4$
4	$\text{Ni}_{.60}\text{Co}_{.30}\text{Fe}_{2.10}\text{O}_4$
5	$\text{Ni}_{.48}\text{Co}_{.45}\text{Fe}_{2.07}\text{O}_4$
6	$\text{Ni}_{.84}\text{Co}_{.27}\text{Fe}_{1.89}\text{O}_4$
7	$\text{Ni}_{.675}\text{Co}_{.48}\text{Fe}_{1.845}\text{O}_4$
8	$\text{Ni}_{.81}\text{X}'_{.03}\text{Fe}_{2.16}\text{O}_4$
9	$\text{Ni}_{.66}\text{X}'_{.03}\text{Co}_{.15}\text{Fe}_{2.16}\text{O}_4$
10	$\text{Ni}_{.81}\text{X}''_{.03}\text{Fe}_{2.16}\text{O}_4$

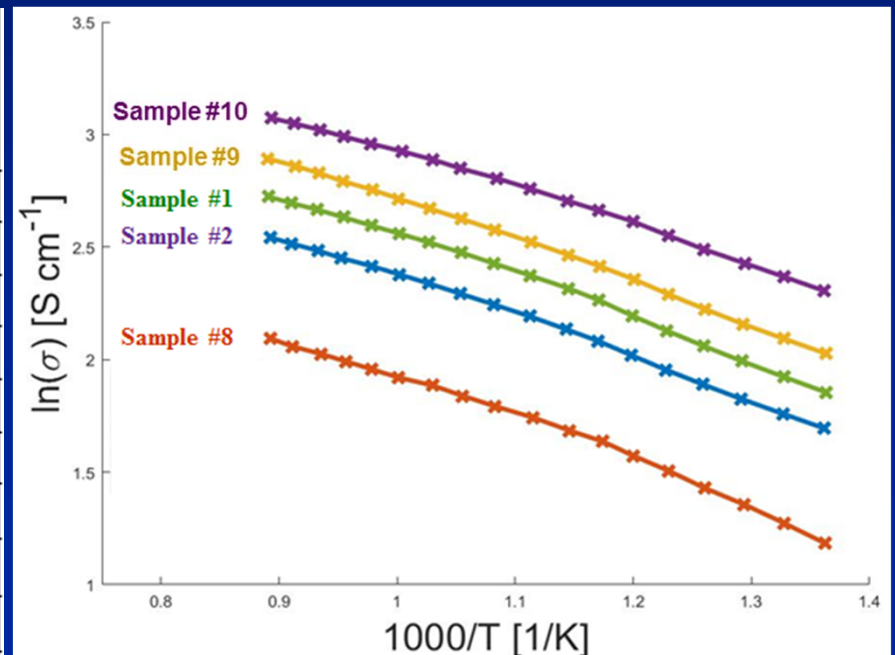


Some Compositions Highlighted on Phase Diagram

Spinel Compositional Optimization in $(\text{Ni,Fe,Co,X})_3\text{O}_4$: Electrical Conductivity and CTE

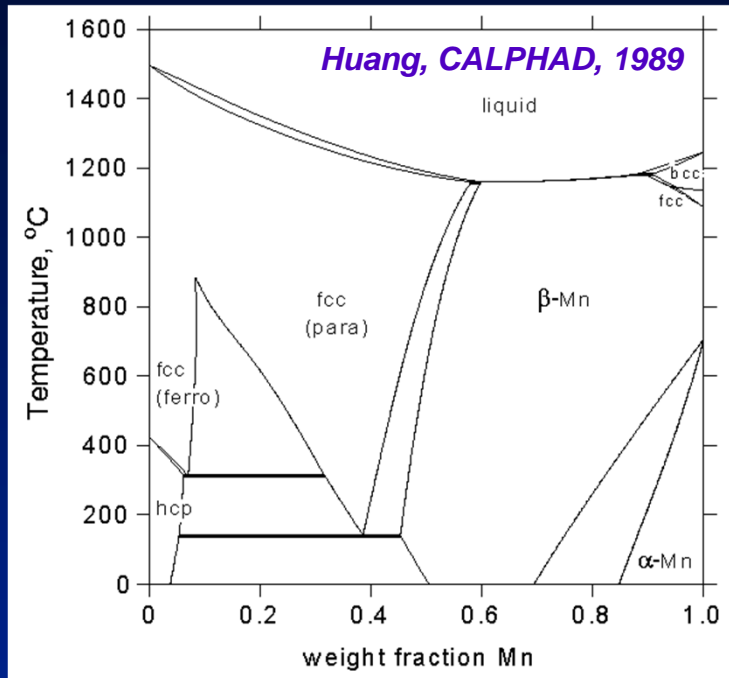
- Regardless of the Co level in the spinel, its Fe level dictated the electrical conductivity, which increased as it became more Fe-excess.
- A combination of Co and X' doping was beneficial in further increasing the spinel conductivity.
- An even higher electrical conductivity was observed in the X''-doped spinel $\text{Ni}_{0.81}\text{X}''_{0.03}\text{Fe}_{2.16}\text{O}_4$.
- Fe/Ni/Co ratio and alloying addition had little effect on CTE ($\sim 12 \times 10^{-6}/^\circ\text{C}$).

Sample #	Composition	Conductivity at 800°C (S/cm)
1	$\text{Ni}_{.84}\text{Fe}_{2.16}\text{O}_4$	14.4
2	$\text{Ni}_{.69}\text{Co}_{.15}\text{Fe}_{2.16}\text{O}_4$	12.0
3	$\text{Ni}_{.72}\text{Co}_{.15}\text{Fe}_{2.13}\text{O}_4$	10.9
4	$\text{Ni}_{.60}\text{Co}_{.30}\text{Fe}_{2.10}\text{O}_4$	7.0
5	$\text{Ni}_{.48}\text{Co}_{.45}\text{Fe}_{2.07}\text{O}_4$	5.1
6	$\text{Ni}_{.84}\text{Co}_{.27}\text{Fe}_{1.89}\text{O}_4$	1.4
7	$\text{Ni}_{.675}\text{Co}_{.48}\text{Fe}_{1.845}\text{O}_4$	2.5
8	$\text{Ni}_{.81}\text{X}'_{.03}\text{Fe}_{2.16}\text{O}_4$	7.6
9	$\text{Ni}_{.66}\text{X}'_{.03}\text{Co}_{.15}\text{Fe}_{2.16}\text{O}_4$	16.9
10	$\text{Ni}_{.81}\text{X}''_{.03}\text{Fe}_{2.16}\text{O}_4$	21.1



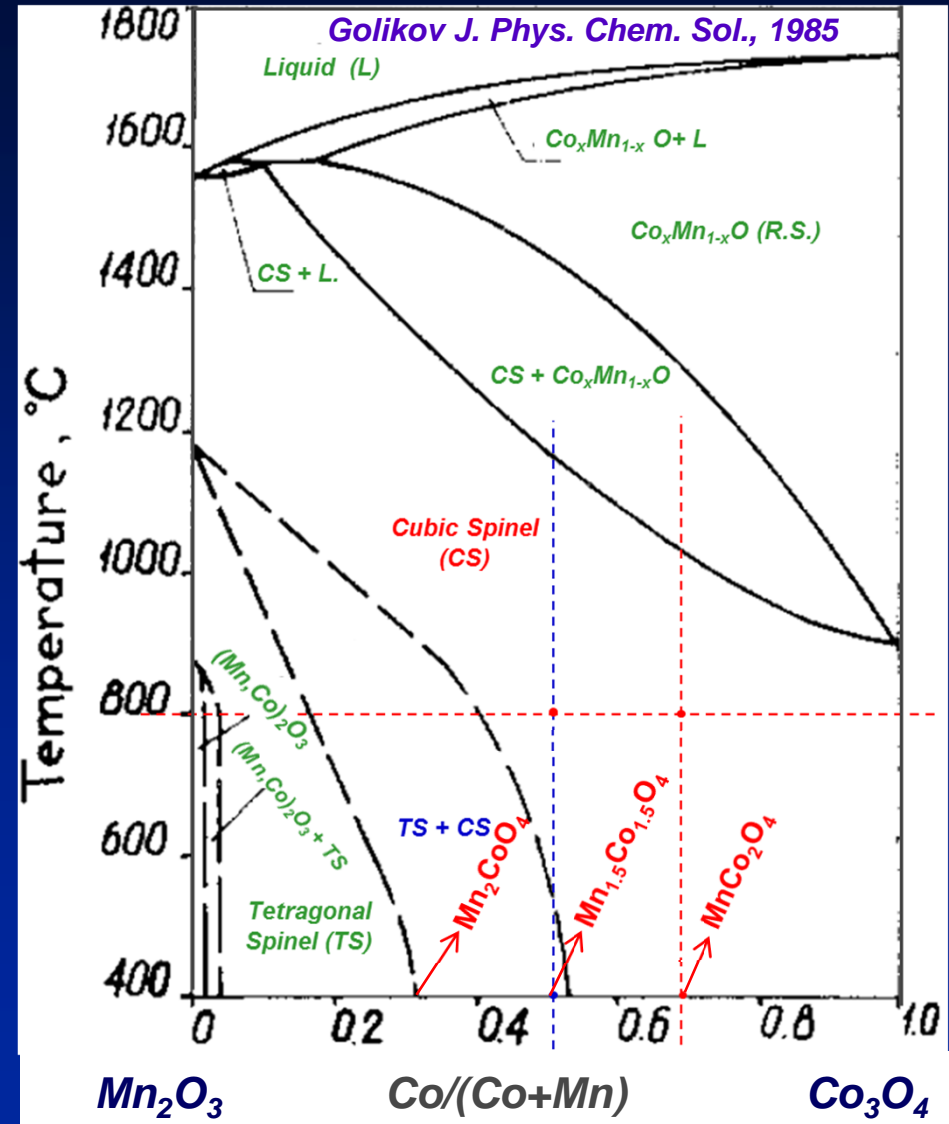
Conductivity as a Function of Temperature 11

Phase Equilibria in $\text{Mn}_2\text{O}_3\text{-Co}_3\text{O}_4$ System



Phase Diagram of the Co-Mn System

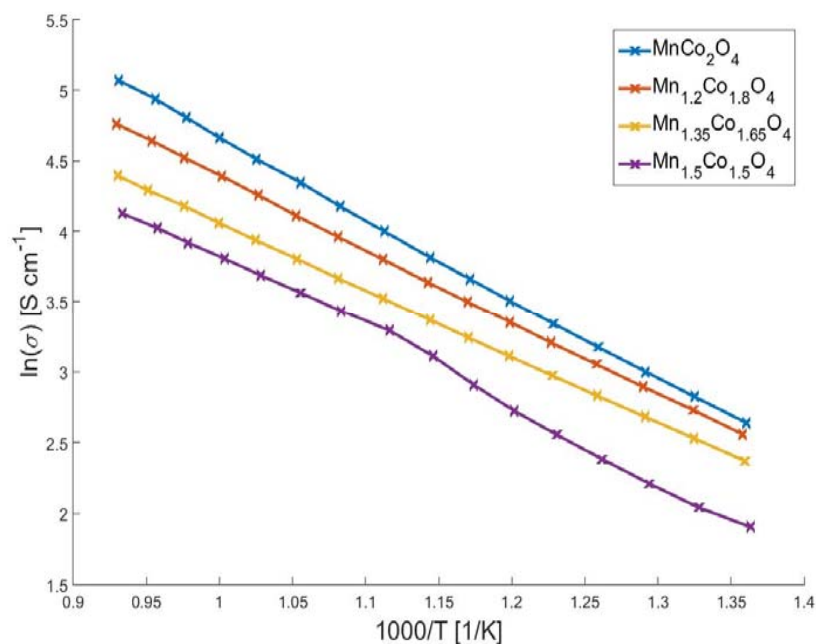
- Some controversies exist for the $\text{Mn}_2\text{O}_3\text{-Co}_3\text{O}_4$ system.
- Two most important compositions in the $(\text{Mn,Co})_3\text{O}_4$ spinel system are:
 - ✓ MnCo_2O_4 : CS at both 800 and 20°C;
 - ✓ $\text{Mn}_{1.5}\text{Co}_{1.5}\text{O}_4$: CS at 800°C and TS + CS at 20°C.



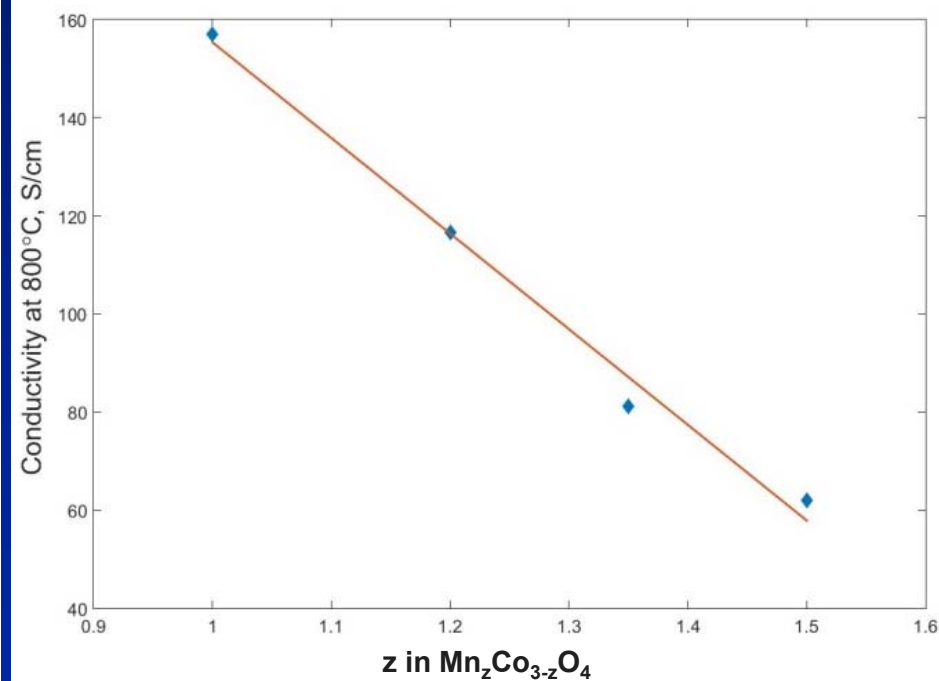
Phase Diagram of the Co-Mn-O System in Air

Spinel Compositional Optimization in $(\text{Mn},\text{Co},\text{X})_3\text{O}_4$: Electrical Conductivity of $\text{Mn}_z\text{Co}_{3-z}\text{O}_4$

- A range of electrical conductivity and CTE has been reported for both MnCo_2O_4 and $\text{Mn}_{1.5}\text{Co}_{1.5}\text{O}_4$. Some data are contradictory to each other.
- As Mn in $\text{Mn}_z\text{Co}_{3-z}\text{O}_4$ increased from $z = 1.0$ (i.e., MnCo_2O_4) to $z = 1.5$ (i.e., $\text{Mn}_{1.5}\text{Co}_{1.5}\text{O}_4$), the electrical conductivity of the spinel decreased.
- A change in activation energy for electrical conduction was observed for $\text{Mn}_{1.5}\text{Co}_{1.5}\text{O}_4$, likely due to the phase transition in this spinel.



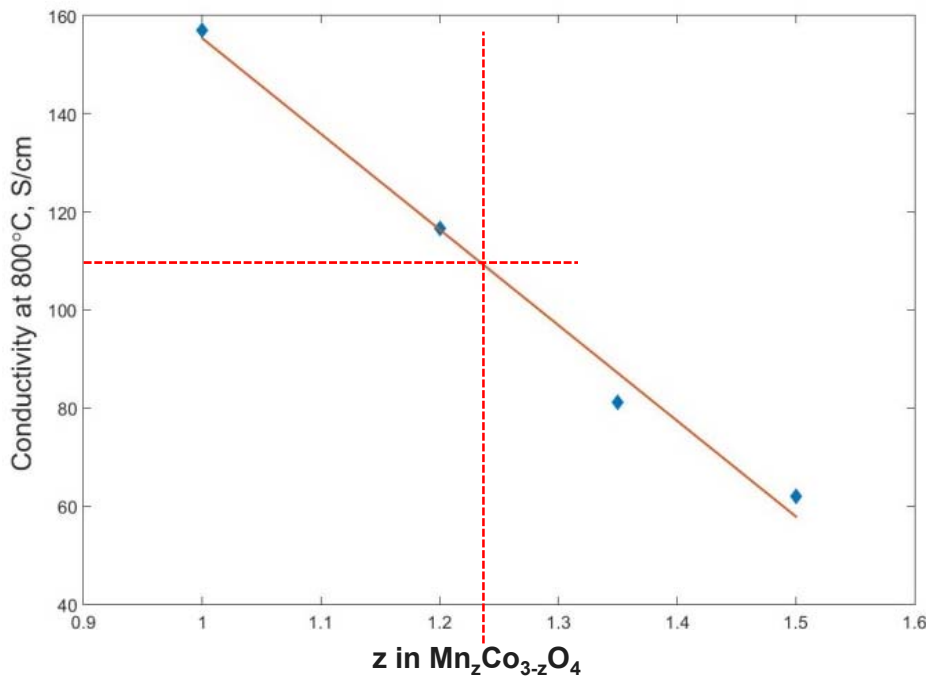
Electrical conductivity vs. Temperature



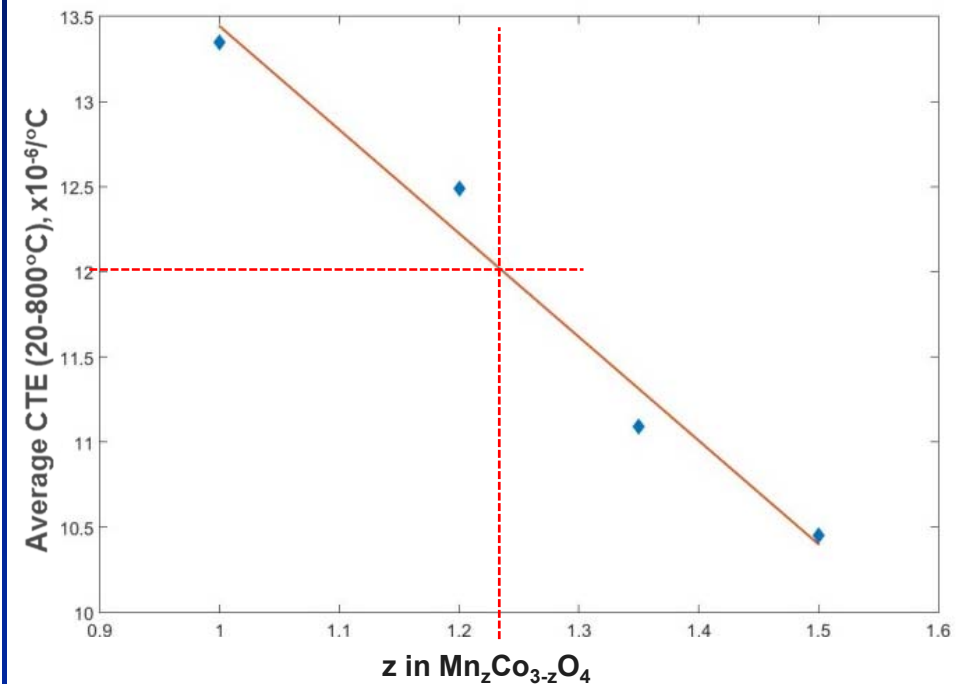
Electrical conductivity at 800°C in Air

Spinel Compositional Optimization in $(\text{Mn},\text{Co},\text{X})_3\text{O}_4$: Average CTE of $\text{Mn}_z\text{Co}_{3-z}\text{O}_4$

- As Mn in $\text{Mn}_z\text{Co}_{3-z}\text{O}_4$ increased from $z = 1.0$ (i.e., MnCo_2O_4) to $z = 1.5$ (i.e., $\text{Mn}_{1.5}\text{Co}_{1.5}\text{O}_4$), the CTE of the spinel decreased.
- A change in the slope of thermal expansion curve for $\text{Mn}_{1.5}\text{Co}_{1.5}\text{O}_4$ is related to the phase transition in this spinel.
- The spinel $\text{Mn}_{1.23}\text{Co}_{1.77}\text{O}_4$ will have a CTE of $12.0 \times 10^{-6}/^\circ\text{C}$ and a conductivity of 110 S/cm at 800°C – likely a better coating choice.



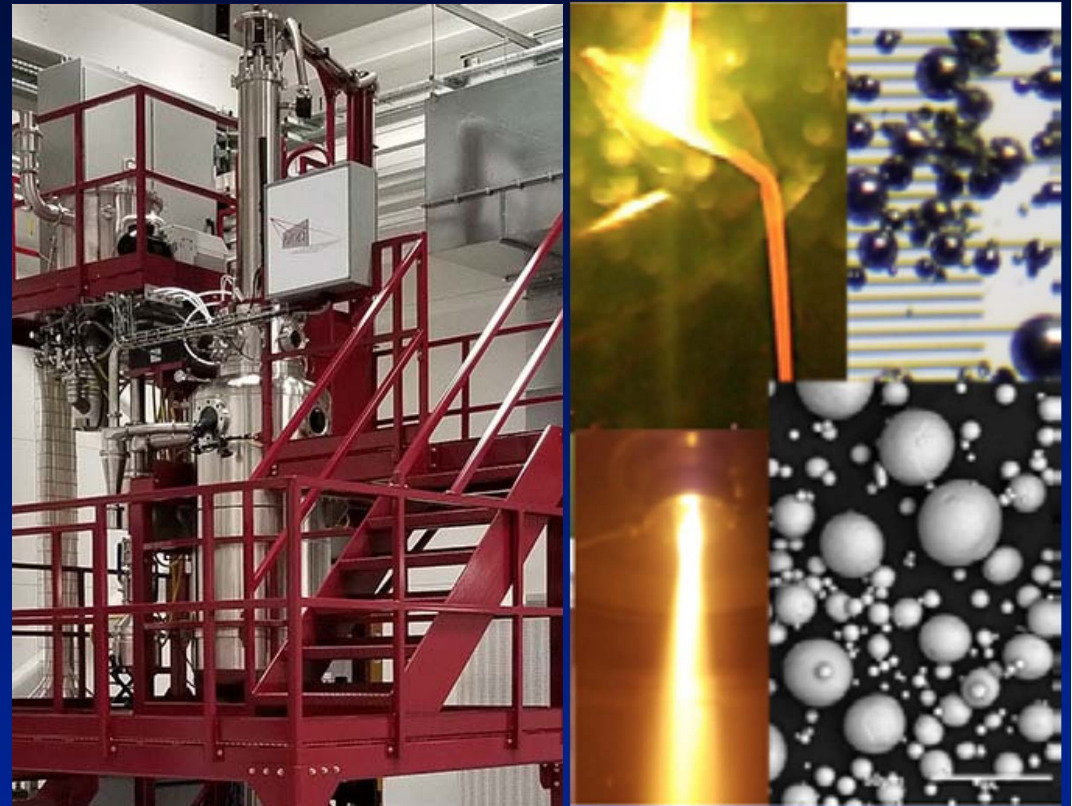
Electrical conductivity at 800°C in Air



Average CTE vs. Spinel Composition

Gas Atomization of the Optimization Alloys

- Based on the phase constitution, electrical conductivity, and CTE, a number of Fe-Ni-Co-X and Mn-Co-X precursor alloy compositions were selected for the powder preparation.
- The powders with the desired composition and particle size were manufactured using a semi-industrial gas atomizer.



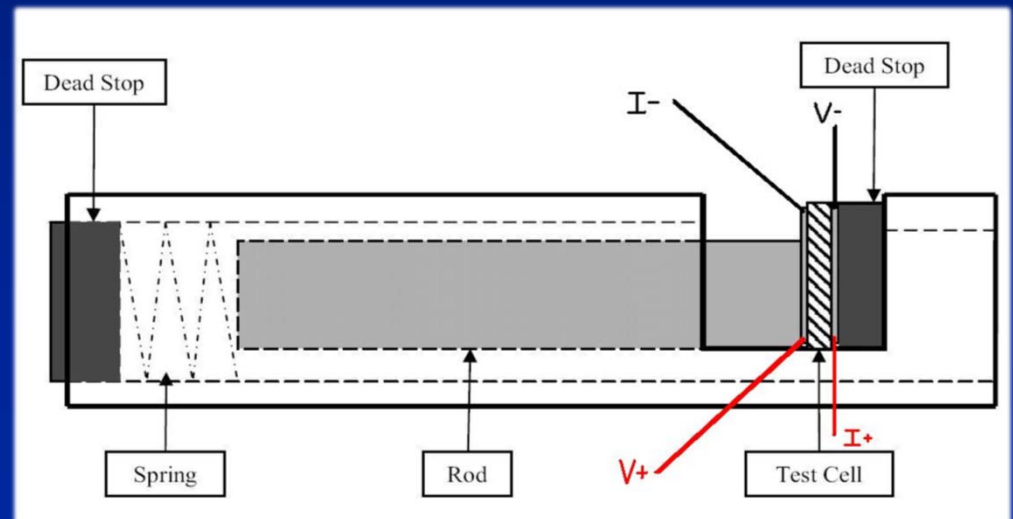
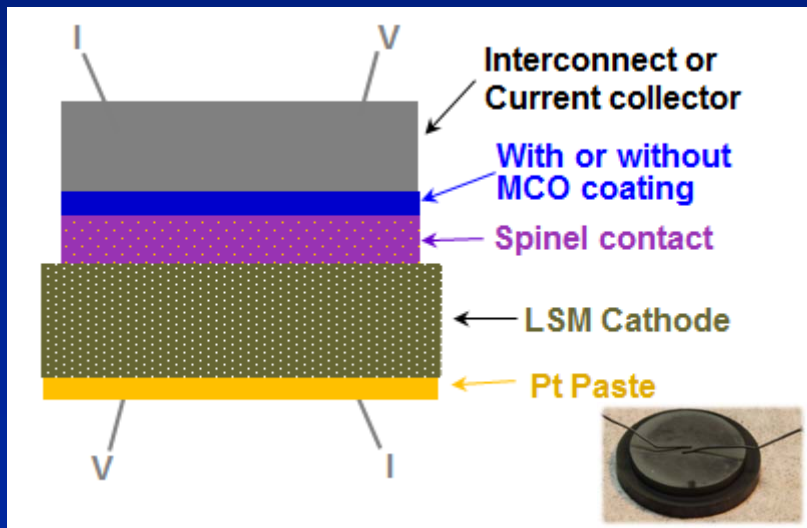
Gas Atomization System

- Chemical analysis of the collected powders was conducted at Dirats Lab – a close match with the targeted compositions was achieved.

TTU is currently in process of acquiring a lab-scale gas atomizer for alloy powder making under a DoD DURIP project.

Area-Specific Resistance (ASR) Measurement

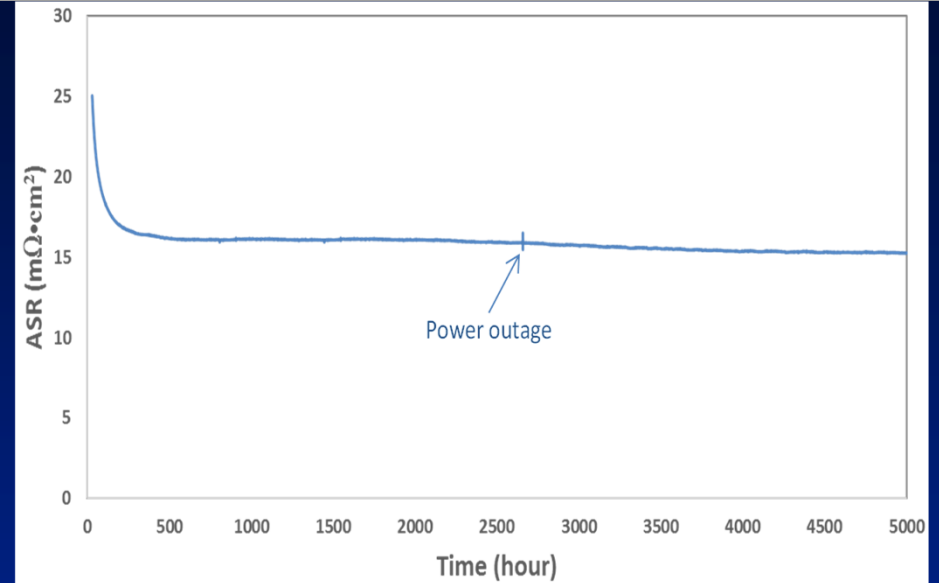
- A number of test cells were constructed, with the spinel-forming contact precursor layer sandwiched between the ferritic alloy [AISI 441, Crofer 22 APU, or $(\text{Mn},\text{Co})_3\text{O}_4$ (MCO)-coated ZMG230G10] and the LSM cathode.
- The test cells were spring-loaded and the ASR change during either isothermal or cyclic exposure at 800°C in air was monitored using a special 6-cell test rig.



Schematic of the ASR Test Cell and Test Configuration

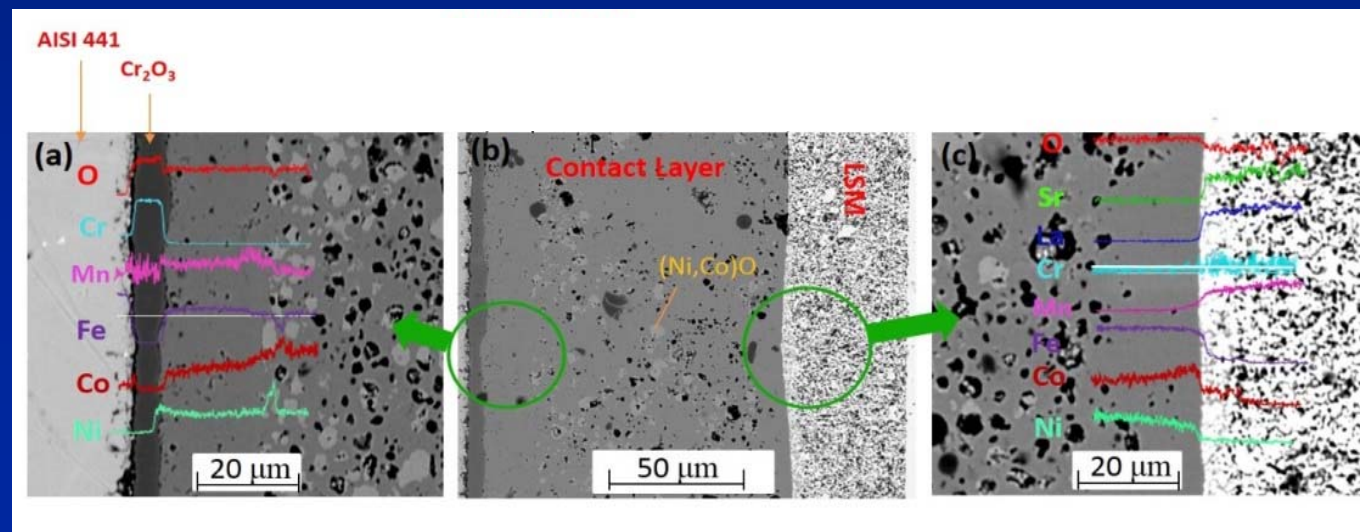
Cell ASR with an Fe-Ni-Co Based Alloy Contact Precursor

- After initial sintering at 900°C for 2 h, the ASR for AISI 441/contact /LSM cell with the Fe-Ni-Co-X alloy precursor was very stable, with an ASR of about 15-17 mΩ·cm² during 5000-h isothermal exposure at 800°C in air.
- The contact layer effectively blocked outward diffusion of Cr from the un-coated AISI 441.



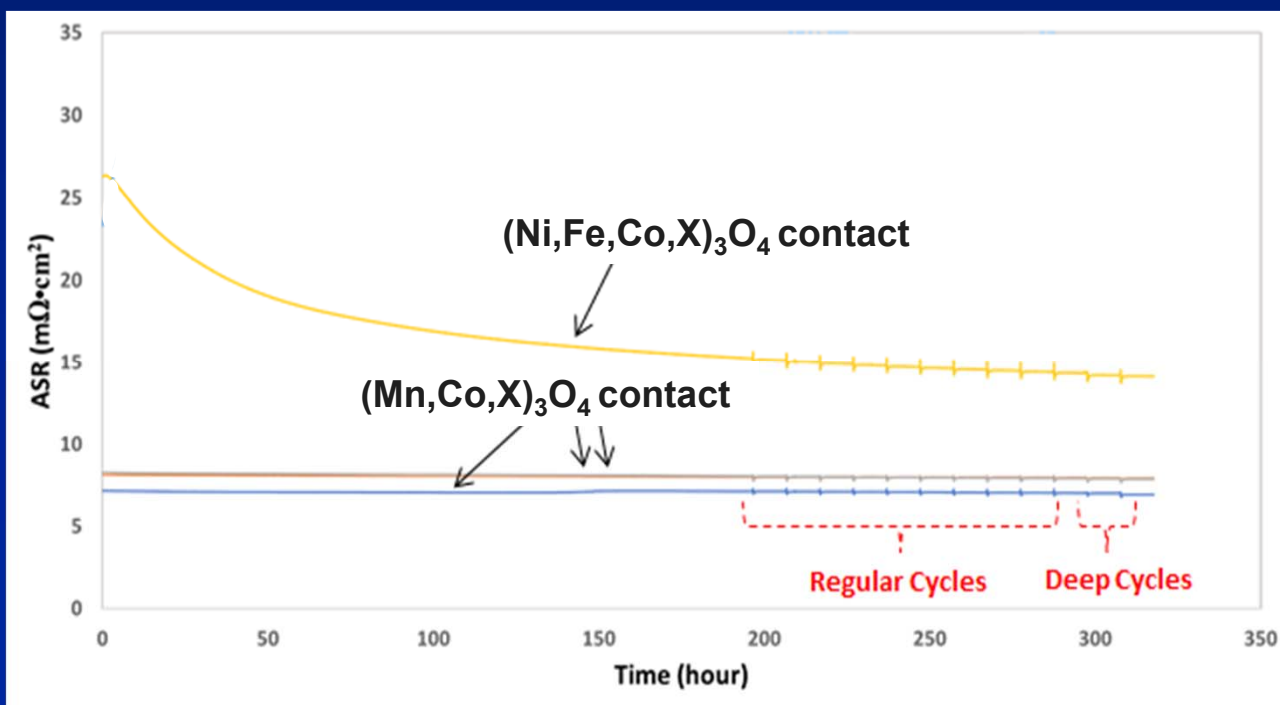
Cell ASR at 800°C during Isothermal Exposure

Cross-sectional View of the Test Cell with EDS Line-scan Results



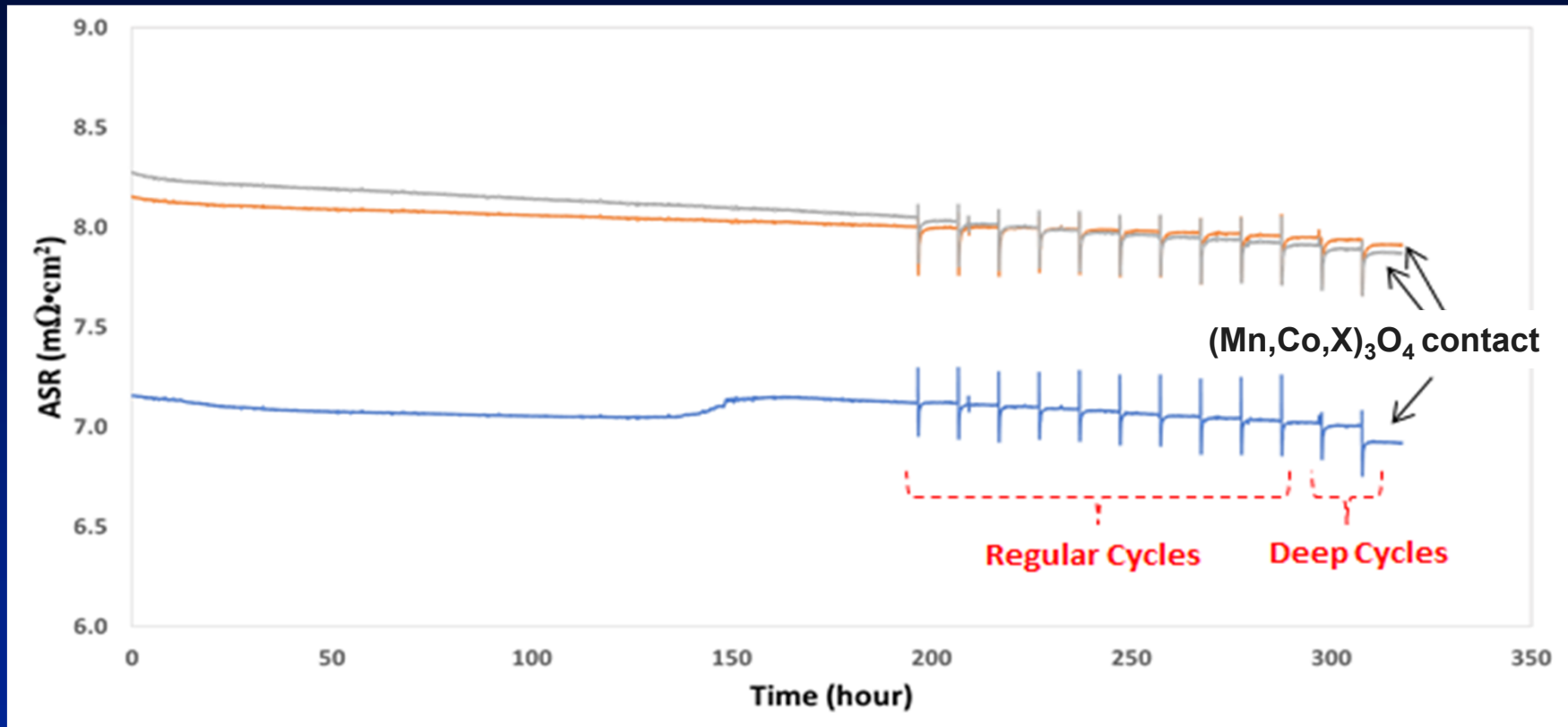
Cell ASR with an $(\text{Mn,Co,X})_3\text{O}_4$ -Forming Precursor

- After initial sintering at 900°C for 2 h, the MCO-precoated ZMG230G10 /contact/LSM cells with the $(\text{Ni,Fe,Co,X})_3\text{O}_4$ / $(\text{Mn,Co,X})_3\text{O}_4$ -forming precursors were isothermally exposed at 800°C for 200 h, followed by 10 regular cycles (cooling to 250°C) and 2 deep cycles (cooling to 20°C).
- Compared to the $(\text{Ni,Fe,Co,X})_3\text{O}_4$ -forming precursor, the $(\text{Mn,Co,X})_3\text{O}_4$ -forming precursor led to lower, more stable ASR values (about $7\text{-}9\text{ m}\Omega\cdot\text{cm}^2$ at 800°C) for the test cells.



Cell ASR vs. Time for Two Different Contact Materials. (Each regular cycle consisting of cooling from 800°C to 250°C , re-heating to 800°C , and then holding at 800°C for 10 h, while during each deep cycle, the cell was cooled to room temperature.)

Stable, low ASR was obtained for the MCO-precoated ZMG230G10/contact/LSM cells with the $(\text{Mn,Co,X})_3\text{O}_4$ contact

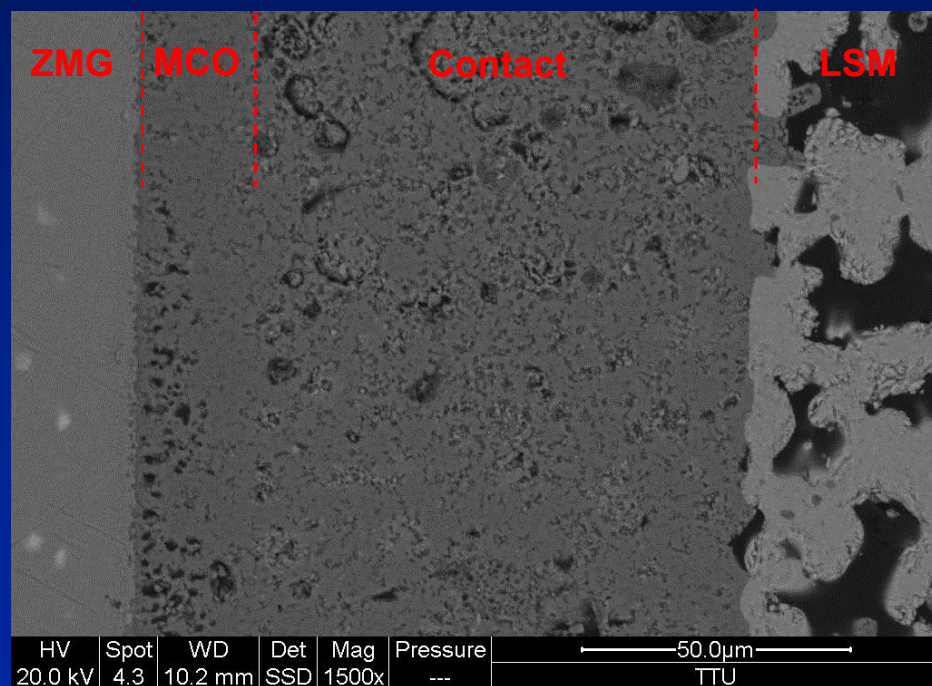


Expanded View of Cell ASR vs. Time for $(\text{Mn,Co,X})_3\text{O}_4$ -Contacted Cells

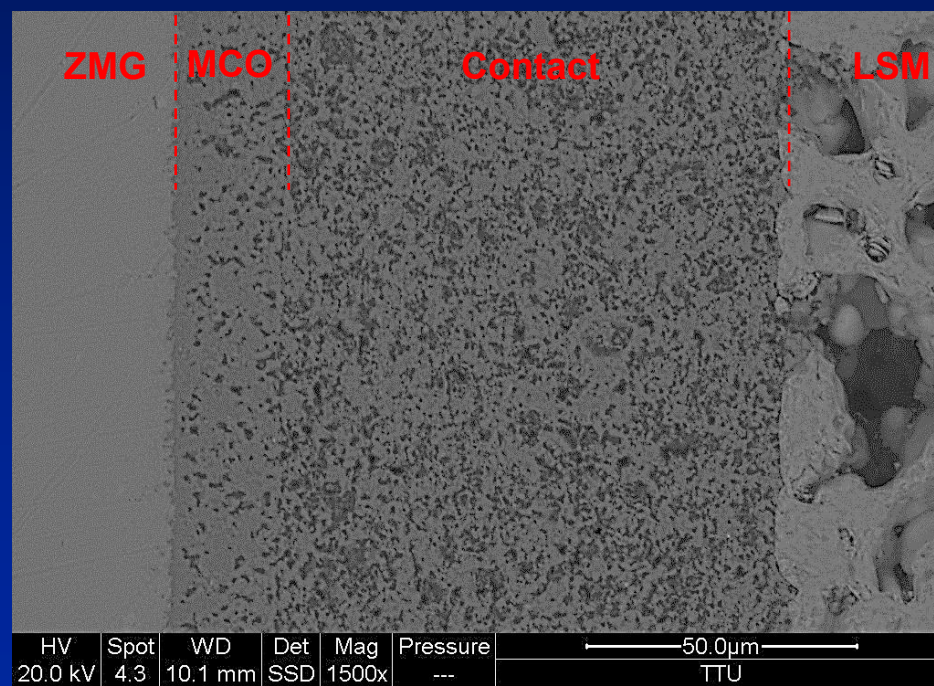
- Very stable, repeatable ASR data was obtained, due to the excellent chemical compatibility between the different components;
- The negligible effect of thermal cycling on the ASR behavior is a result of good matching in CTE between these components.

Cross-sectional View of Tested Cells

- For both cases, a porous contact layer was formed between the coated alloy and the porous cathode. No cracking or delamination near the contact zone was observed.
- Negligible interactions between the contact layer with the MCO coating or the LSM cathode were noticed.



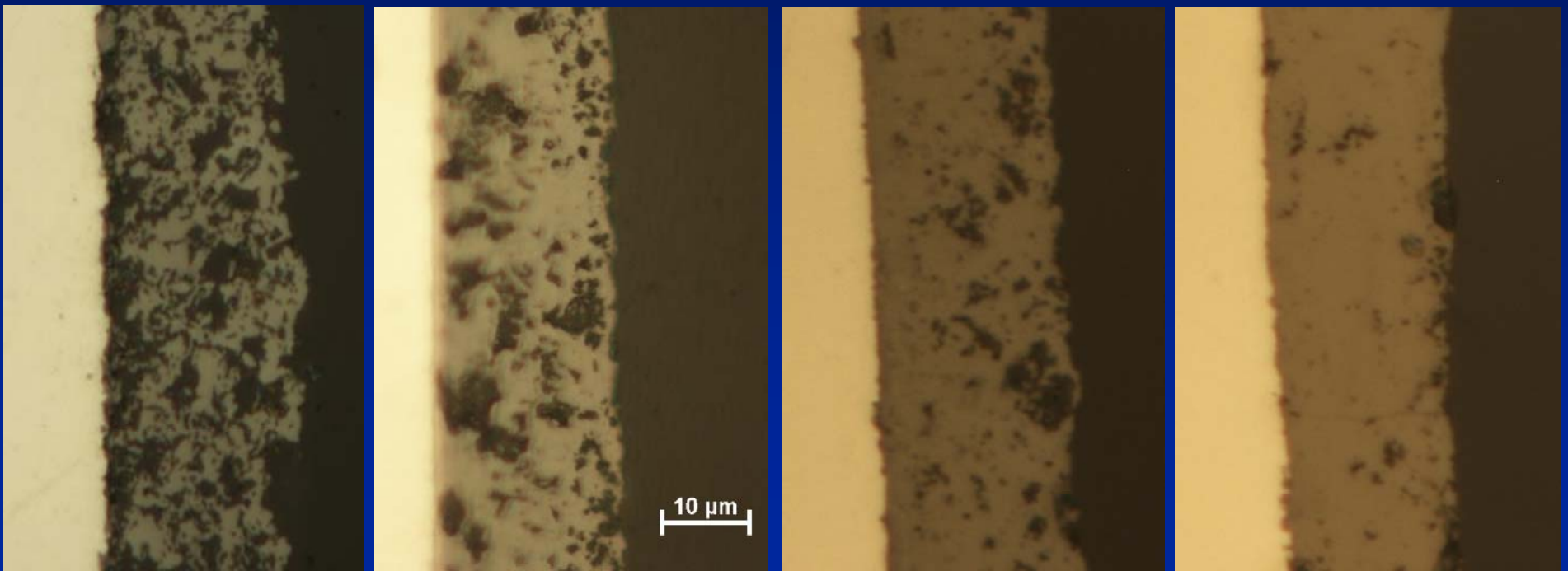
Cross-sectional View of Tested Cell with the $(\text{Ni,Fe,Co,X})_3\text{O}_4$ Contact



Cross-sectional View of Tested Cell with the $(\text{Mn,Co,X})_3\text{O}_4$ Contact

EARS Processing of Dense MCO Coatings

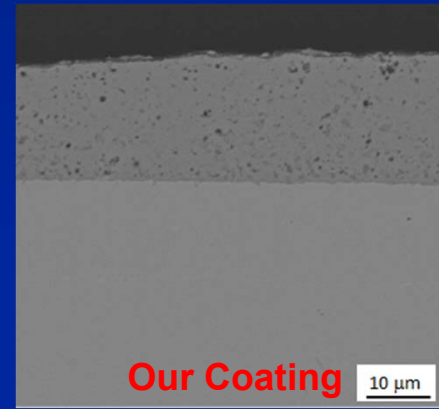
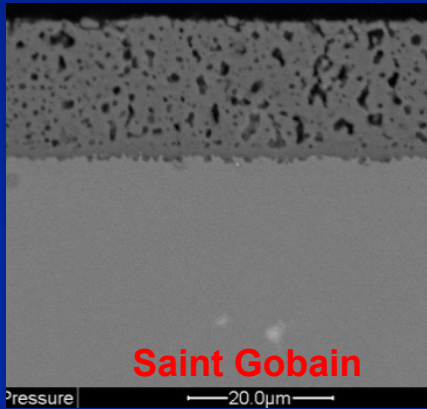
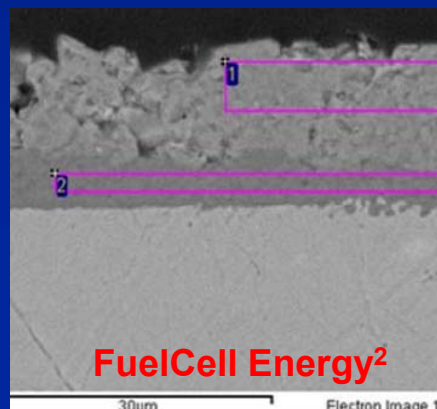
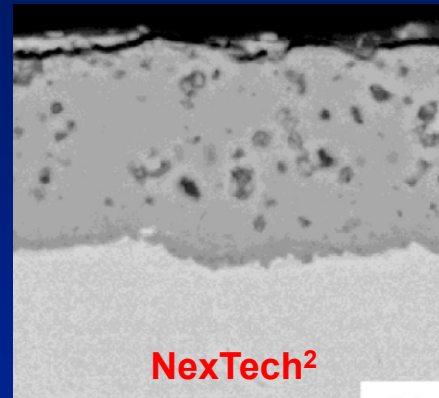
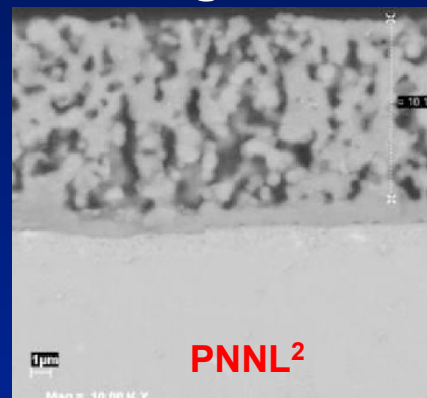
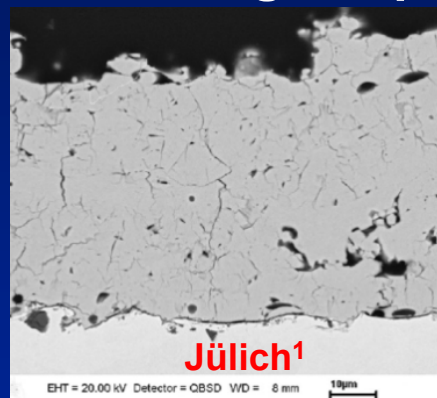
- Reactive sintering of a dense MCO coating via EARS has been explored and initial results are very encouraging:
 - By controlling the composition/shape/size/size distribution/initial packing density of the metallic precursor powders, a dense spinel layer was obtained after thermal conversion at 900°C for 2 h in air.



Improvement in Quality of TTU's Reactive Sintered MCO Coatings on Crofer 22 APU

Comparison of Our Coating with the State-of-the-Art

- Current MCO coating processes typically involve costly equipment, high processing temperatures ($> 900^{\circ}\text{C}$) and/or a reduction treatment.
- Our EARS process offers a potentially better MCO coating quality.
- The EARS-derived coating does not require a reduction treatment or a sintering temperature higher than 900°C .

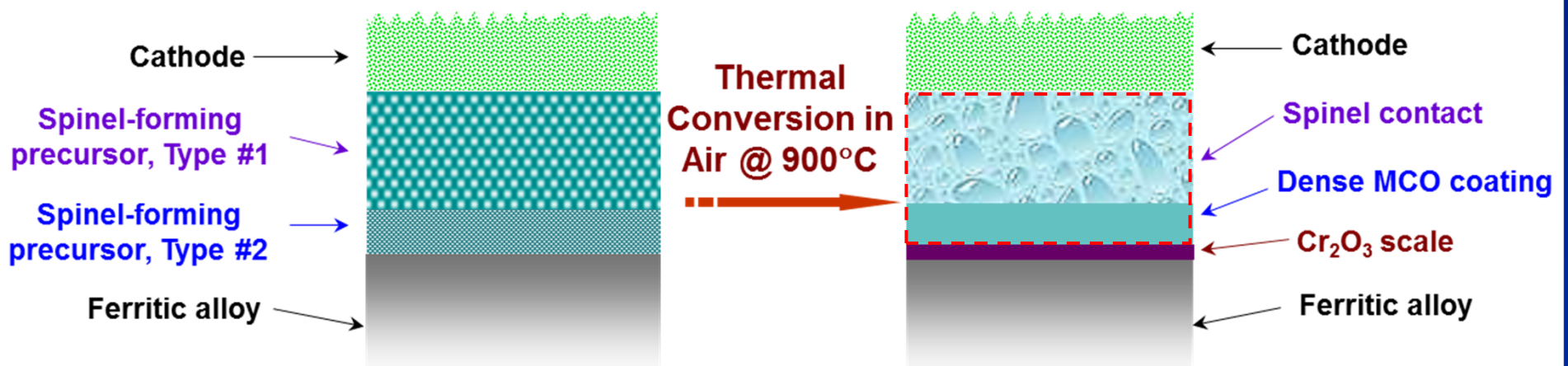


¹R. Vaßen et al.,
Surf. & Coat.
Tech., 2016;

²Ghezal-Ayagh,
SECA Coal-Based
Systems – Final
Report, 2014

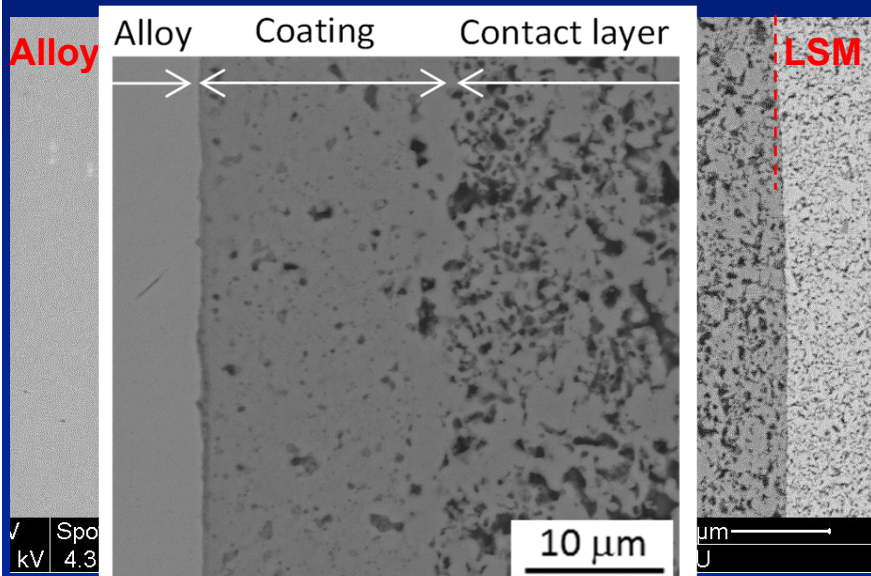
Co-sintering of Coating/Contact Dual-Layer Structure: Proposed Approach

- To lower the interfacial ASR at the alloy/contact interface, improve the contact quality, and reduce the coating and contact processing cost, co-sintering of the coating and the contact layer during initial stack firing/operation is also explored, utilizing two different metallic precursors:
 - Two spinel-forming precursors (Type #1 – for the contact layer and Type #2 – for the dense MCO coating) will be employed;
 - Reactive co-sintering in air at a sintering temperature of 900°C will be utilized for simultaneous formation of the dual-layer structure.

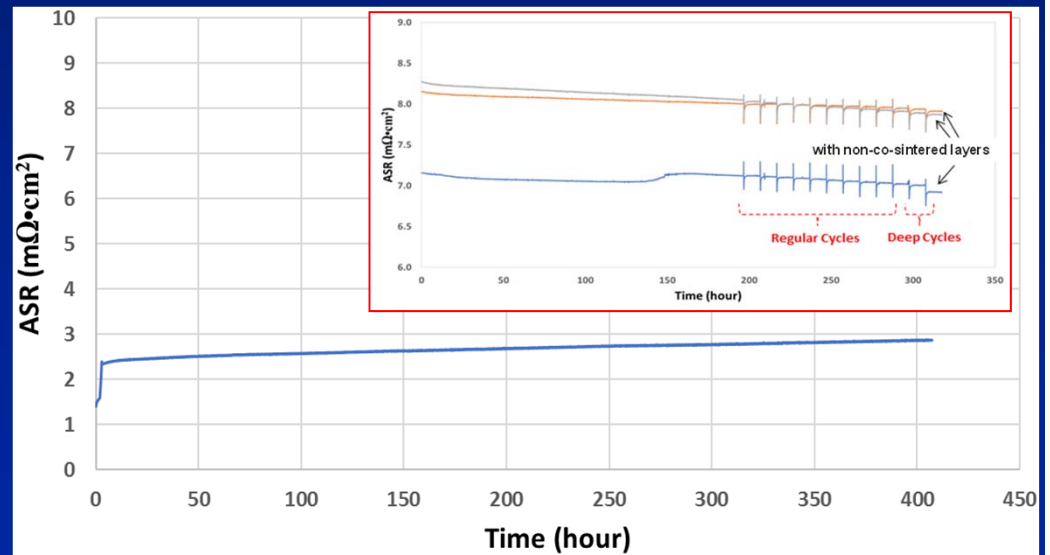


Initial Results on Co-sintering of Coating/Contact Layers

- After screen printing the spinel-forming coating/contact precursor layers on Crofer 22 APU, the alloy/coating/contact /LSM cell was co-sintering in air at 900°C for 2 h.
- A highly dense MCO coating layer and a porous contact layer were obtained, both of which were well sintered.
- Our co-sintered dual-layer structure led to better ASR performance than the non-co-sintered ones.

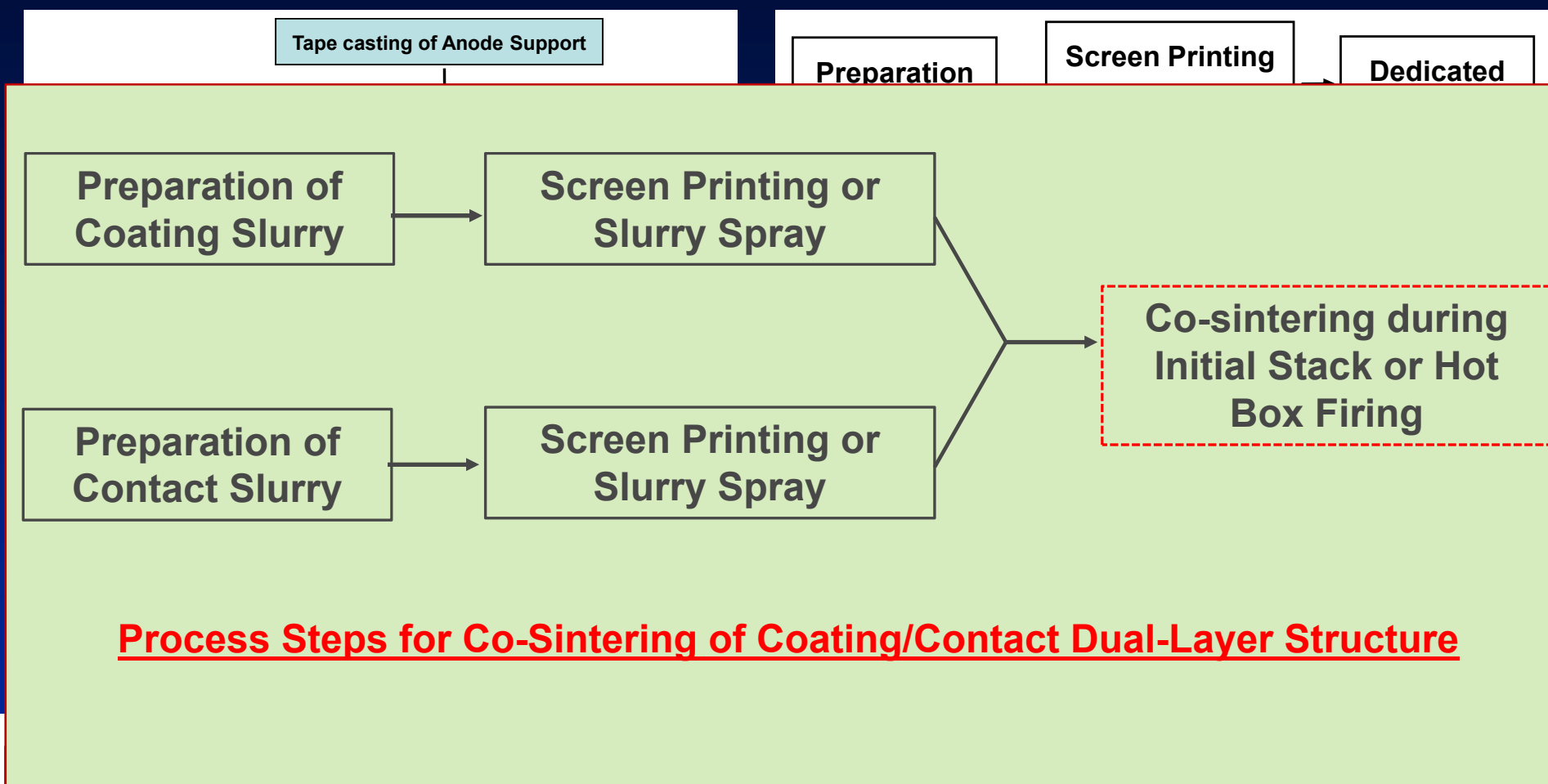


Cross-sectional View of Co-sintered Dual-layer Structure

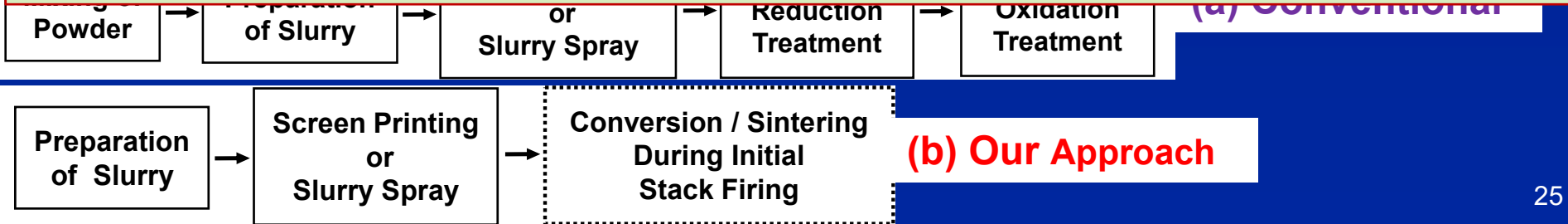


Cell ASR vs. Time with the Co-sintered Dual-layer Structure between Crofer 22 APU & LSM²⁴

Cost Analysis – Simplified Synthesis of Contact Layer and Interconnect Coating for ASC-SOFC Stacks



Process Steps for Co-Sintering of Coating/Contact Dual-Layer Structure



Concluding Remarks

- Several compositions in the $(\text{Ni,Fe,Co,X})_3\text{O}_4$ and $(\text{Mn,Co,X})_3\text{O}_4$ systems have been identified for SOFC contacting applications, based on considerations of phase constitution, electrical conductivity, CTE, etc.
- A number of Ni-Fe-Co and Mn-Co based precursor alloy powders have been prepared via gas atomization.
- Low-cost, EARS-processed $(\text{Ni,Fe,Co})_3\text{O}_4$ - and $(\text{Mn,Co})_3\text{O}_4$ -based contact layers with promising ASR performance have been successfully demonstrated.
- By controlling the metallic precursor powder composition, size, size distribution, and initial powder packing density, a dense MCO coating have been synthesized for protecting the interconnect or current collector alloys.
- Co-sintering of a dual-layer structure with a dense spinel layer as coating and a porous layer as contact can be achieved by utilizing two tailored metallic precursors.

Acknowledgments

- **U. S. Department of Energy - National Energy Technology Laboratory, Solid Oxide Fuel Cell Prototype System Testing and Core Technology Development Program, Award No. DE-FE0031187; Project Manager: Dr. Patcharin Burke**
- **Allen Yu, Joseph Simpson, David Chesson, and Brian Bates, TTU**
- **Dr. Hossein Ghezel-Ayagh, FuelCell Energy, Inc.**
- **Dr. John Pietras and his team at Saint Gobain**

Project Milestones

Milestone Title/Description	Planned Start Date	Planned Completion Date	Actual Completion Date	Verification Method	Status
Revised PMP	10/10/2017	10/30/2017	10/23/2017	PMP file	Completed
Kickoff Meeting	10/30/2017	12/29/2017	11/29/2017	Presentation file	Completed
Compositional optimization of Precursor alloy	11/01/2017	06/30/2018	06/28/2018	Optimal Fe/Ni/Co and other alloy additions are identified.	Completed
Preparation of the optimized alloy powder	11/15/2017	09/31/2018	09/20/2018	Atomization of one alloy powder is completed.	Completed
Demonstration of long-term cell ASR stability with the new contact	01/01/2018	06/30/2019	02/20/2019	The ASR stability is demonstrated successfully for about 5,000 h.	Completed
Demonstration of stack performance stability with 1-cell stack testing	04/02/2018	07/31/2019		Stack performance stability testing for \geq 1,000 h is completed at industrial site.	In progress
Cost analysis and commercialization feasibility	07/01/2019	09/31/2019		Cost analysis and scale-up assessment are completed.	Just started